Final Report

Project Title: Fabrication of transparent CNT films for OLED application
Project Period: 2008.02.1 ~ 2009.02.28
Budjet: USD 25,000
P.I.: Professor Soonil Lee (Field of Study, Physics/NT)
Division of Energy Systems research, Ajou University

Summary

We optimized the process to prepare SWCNT solutions with the good degree of dispersion of individually isolated SWCNTs and very thin SWCNT bundles. Our SWCNT-dispersion solutions are so stable that they can be stored and used repeatedly for some period of time. The thin-film casting by spin-coating resulted in SWCNT films with uniform sheet resistance and visible-light transmittance. With the control of the spin-coating conditions we were able to control the thickness, sheet resistance and visible-light transmittance with the general trend that the reduction of sheet resistance requires the sacrifice of visible transmittance. Further reduction of the sheet resistance with a limited sacrifice of visible-light transmittance was achieved through the treatment of SWCNT films with nitric-acid. For example, the sheet resistance of 85 Ω/sq and the transmittance of 80% (@ λ = 550 nm) were measured from the 40-nm-thick SWCNT on a PET substrate. Moreover, the repetition of the HNO_3-treatment and thermal annealing has the extra benefit of the improved adhesion of SWCNT films to substrates. Another process that we developed for more efficient reduction of the sheet resistance was the combination treatment of SWCNT films with HNO_3 and $SOCl_2$. This new process turned out to be more stable against undesired increase of the sheet resistance due to the inevitable heating that the SWCNT would experience during the OLED fabrication. It appears that the doping and de-doping effects are more prominent in the combination treatment with HNO_3 and $SOCl_2$, as evidenced by the suppression and recovery of the van Hove singularities in response to the combination treatment and heating. More evidence for the anodic doping (electron withdrawal) due to the combination treatment was found from the resonance Raman scattering. The distinct Raman modes of the some semiconducting SWCNTs that appeared strong because of the resonance of the excitation energy (1.15 eV) with the S_{22} transition became substantially weak after the HNO_3-$SOCl_2$ combination treatment. One of the key process steps for OLED fabrication on SWCNT electrodes is the anode patterning. Through systematic investigation of photolithography and oxygen plasma etching processes, we optimized process parameters to pattern the SWCNT films into desired anode patterns without the contamination, delamination, and sheet-resistance increase. Another important issue related to the SWCNT anode is how to overcome the surface roughness: in particular, very large peak-to-valley height variation. We handled this problem by using a PEDOT:PSS hole-injection layer for the planarization. OLEDs with the structure of SWCNT-anode/PEDOT:PSS(90 nm)/NPB(200 nm)/Alq_3(40 nm)/LiF(1 nm)/Al(100 nm) were successfully fabricated. The operation of such a device showed that the performance of a green-emitting OLED based on the SWCNT anode is comparable to that of more convention green-emitting OLEDs fabricated on ITO anodes.

Report Documentation Page

Form Approved
OMB No. 0704-0188

1. REPORT DATE	2. REPORT TYPE	3. DATES COVERED
04 FEB 2010	**FInal**	**02-02-2008 to 28-02-2009**

4. TITLE AND SUBTITLE	5a. CONTRACT NUMBER
Fabrication of transparent CNT films for OLED application	**FA48690814033**
	5b. GRANT NUMBER
	5c. PROGRAM ELEMENT NUMBER
6. AUTHOR(S)	5d. PROJECT NUMBER
Soon Il Lee	5e. TASK NUMBER
	5f. WORK UNIT NUMBER
7. PERFORMING ORGANIZATION NAME(S) AND ADDRESS(ES)	8. PERFORMING ORGANIZATION REPORT NUMBER
Ajou University,San 5, Woncheon-dong, Yeongtong-gu,Suwon 443-749,Korea (South),KR,443-749	**N/A**
9. SPONSORING/MONITORING AGENCY NAME(S) AND ADDRESS(ES)	10. SPONSOR/MONITOR'S ACRONYM(S)
AOARD, UNIT 45002, APO, AP, 96337-5002	**AOARD**
	11. SPONSOR/MONITOR'S REPORT NUMBER(S)
	AOARD-084033

12. DISTRIBUTION/AVAILABILITY STATEMENT
Approved for public release; distribution unlimited

13. SUPPLEMENTARY NOTES
We optimized the process to prepare SWCNT solutions with the good degree of dispersion of individually isolated SWCNTs and very thin SWCNT bundles. Our SWCNT-dispersion solutions are so stable that they can be stored and used repeatedly for some period of time. The thin-film casting by spin-coating resulted in SWCNT films with uniform sheet resistance and visible-light transmittance.

14. ABSTRACT
With the control of the spin-coating conditions we were able to control the thic kness, sheet resistance and visible-light transmittance with the general trend t hat the reduction of sheet resistance requires the sacrifice of visible transmit tance. Further reduction of the sheet resistance with a limited sacrifice of vis ible-light transmittance was achieved through the treatment of SWCNT films with nitric-acid. For example, the sheet resistance of 85 /sq and the transmi ttance of 80% (@  = 550 nm) were measured from the 40-nm-thick SWC NT on a PET substrate. Moreover, the repetition of the HNO3-treatment and therma l annealing has the extra benefit of the improved adhesion of SWCNT films to substrates. Another process that we developed for more efficient reduction of the sheet resistance was the combination treatment of SWCNT films with HNO3 and SOCl2. This new process turned out to be more stable against undesired increase of the sheet resistance due to the inevitable heating that the SWCNT would experience during the OLED fabrication. It appears that the doping and de-doping effects are more prominent in the combination treatment with HNO3 and SOCl2, as evidenced by the suppression and recovery of the van Hove singularities in response to the combination treatment and heating. More evidence for the anodic doping (electron withdrawal) due to the combination treatment was found from the resonance Raman scattering. The distinct Raman modes of the some semiconducting SWCNTs that appeared strong because of the resonance of the excitation energy (1.15 eV) with the S22 transition became substantially weak after the HNO3-SOCl2 combination treatment. One of the key process steps for OLED fabrication on SWCNT electrodes is the anode patterning. Through systematic investigation of photolithography and oxygen plasma etching processes, we optimized process parameters to pattern the SWCNT films into desired anode patterns without the contamination, delamination, and sheet-resistance increase. Another important issue related to the SWCNT anode is how to overcome the surface roughness: in particular, very large peak-to-valley height variation. We handled this problem by using a PEDOT:PSS hole-injection layer for the planarization. OLEDs with the structure of SWCNT-anode/PEDOT:PSS(90 nm)/NPB(200 nm)/Alq3(40 nm)/LiF(1 nm)/Al(100 nm) were successfully fabricated. The operation of such a device showed that the performance of a green-emitting OLED based on the SWCNT anode is comparable to that of more convention green-emitting OLEDs fabricated on ITO anodes.

15. SUBJECT TERMS
condensed matter physics, nanoscience & Technology, Carbon nano tubes, Organic Light Emitting Diode (OLED)

16. SECURITY CLASSIFICATION OF:			17. LIMITATION OF ABSTRACT	18. NUMBER OF PAGES	19a. NAME OF RESPONSIBLE PERSON
a. REPORT	b. ABSTRACT	c. THIS PAGE	**Same as Report (SAR)**	**12**	
unclassified	**unclassified**	**unclassified**			

Experimental Details

Procedure to make SWCNT dispersion solutions:

Arc-made SWCNTs (85wt% purity as determined from the TGA result) purchased from Iljin Nanotech were used as a starting material. The SWCNTs were vacuum dried overnight at 100 °C to get rid of water molecules adsorbed on the SWCNT sidewalls. The dried SWCNTs were dispersed in either dichloroethane (DCE) or dichlorobenzene (DCB) through the 9-hour ultrasonic agitation (100 W at 42 kHz). Next, the SWCNT-dispersed solutions were centrifuged at 48,000 g for 30 minutes to induce sedimentation of large SWCNT bundles and any other carbonaceous materials. Decanting the upper portion of the centrifuged solutions, we obtained homogeneous SWCNT-dispersion solutions (typical density of ~0.005 mg/ml).

Procedure to cast SWCNT network Films:

SWCNT-network films were cast on either glass or flexible PET substrates using a spin coater. The number of spin-coating was one of the important process parameters to control the sheet resistance and the visible transmittance of SWCNT films. To cast SWCNT films on PET substrates, proper size PET pieces were attached to glass backing plates using double-sided adhesive tapes to prevent bending and sliding of PET substrates during spin-coating operation. In the case of casting on glass substrates, 3-aminopropyl triethoxysilane was used to improve the adhesion between SWCNT films and the glass substrates. First, 1 wt% solution of 3-aminopropyl triethoxysilane was dropped on the glass substrate and left set for 5 minutes. Next, the excess 3-aminopropyl triethoxysilane solution was removed by spinning and thoroughly rinsing the substrates prior to the SWCNT-film casting.

Procedure to reduce sheet resistance of SWCNT network Films:

Post-treatment with nitric acid was used to reduce the sheet resistance of the SWCNT films without significant reduction of transmittance in visible wavelength range. The SWCNT films on the substrates were first exposed to the saturated HNO_3 fume for 1 hour. Next, the SWCNT films were rinsed thoroughly and baked at 80 $^{\circ}$C under vacuum for 30 minutes. THTHI process was repeated several times to enhance the adhesion between the SWCNT films and substrates. Another method we used to reduce the sheet resistance of the SWCNT films was the treatment with $SOCl_2$. The treatment was also carried out through the controlled exposure of the SWCNT films to the $SOCl_2$ vapor.

Procedure to fabricate and to test OLED on SWCNT electrodes:

The conventional photolithography technique was used to form patterned SWCNT anodes. We note that the exposed areas of the SWCNT films were easily removed by using a radio frequency oxygen-plasma (40 s, 100 mTorr, 100mW), whereas the PR-coated areas remained intact. Acetone-rinsing to remove the protective PR after the reactive ion etching induced no degradation to the SWCNT anodes. For OLED fabrication, we first deposited a PEDOT:PSS layer by spin coating, and then NPB, Alq_3, LiF ,and Al layers were evaporated at the pressure of 1×10^{-6} torr. All the fabrication steps were performed in a glove-box and a thermal evaporator directly connected to it. The fabricated OLEDs were hermetically sealed by glass encapsulations with getters before being taken out from the glove box for current-luminance-voltage measurements.

Results

Preparation of SWCNT dispersion solution and casting of SWCNT Films:

Selection of dispersion medium and ultrasonication conditions, such as power, frequency, and time, are important process parameters to make stable good quality SWCNT dispersion solutions. We note that the preparation of good CNT dispersion solutions, without cutting CNTs too short due to excessive ultrasonication, is essential for the successful fabrication of CNT electrodes with low sheet resistance and high visible-light transmission. Through an extensive search for optimal process conditions, we were able to make dispersion solutions that contained less bundled and individually separated micrometer-scale SWCNTs.

Figure 1(a) that is an AFM image of the SWCNTs transferred to a glass substrate confirms that the dispersion solutions rich in individual SWCNTs was made by agitating the DCE-based SWCNT solution by ultrasonication at 42 kHz and 100W for 9 hours. This AFM image shows that there are many numbers of individually isolated SWCNTs and small size SWCNT bundles ranging from 3 to 6 nm. Through the examination of 160 SWCNTs from the 8 AFM images, sampling 20 SWCNTs from each $5 \times 5\mu m^2$ image, we estimate the average diameter and length of SWCNTs as 2.6±1.96 nm and 1.65±0.68 μm, respectively. Figures 1(b) and 1(c) are typical AFM images of SWCNT films that are fabricated by repeating the spin coating 100 times on glass and PET substrate, respectively. As these figures show, SWCNTs forms a continuous network structure on both substrates, and the root-mean-square (RMS) roughness is about 7-10 nm for both films.

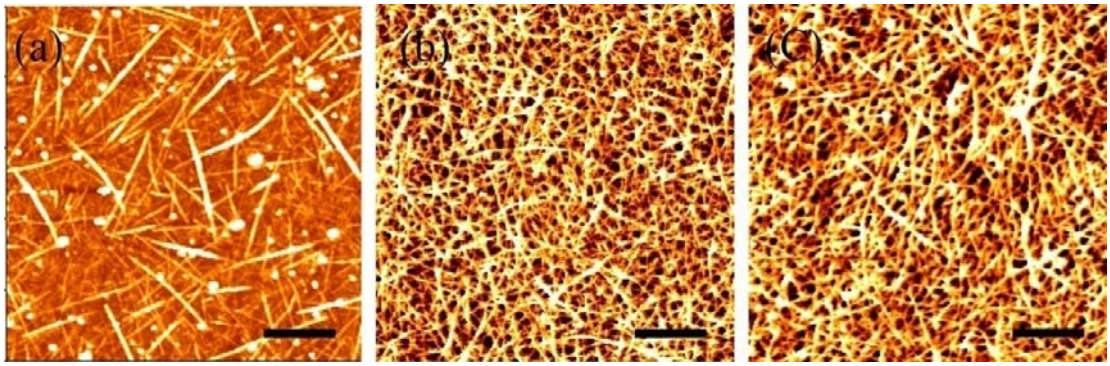

Figure 1: Typical AFM images of SWCNT films on substrates: (a) single spin coating using dispersion, and after repeating spin coating 100 times on (b) glass and (c) PET. The scale bar is 1 μm.

Sheet resistance and visible-light transmittance of as-made SWCNT films:

Figure 2 shows transmittance (T) for visible lights and sheet resistance (R_s) of a series of SWCNT films spin-coated 20, 40, and 100 times, respectively, on glass and PET substrates. We note that even when spin-coating was repeated for 100 times, the transmission at the wavelength of 550 nm remains over 83% on both substrates, but that there is a significant difference in sheet resistance between SWCNT films on two different substrates: T = 83% and R_s = 320 ± 17 Ω/sq on the glass, and T = 89% and R_s = 638 ± 36 Ω/sq on the PET substrates, respectively. The different sheet-resistance values can be attributed to the difference in SWCNT networking on two different types of substrates. It seems that the SWCNT-dispersion solution wetted the glass substrates better, compared to the PET ones, and that consequently, SWCNTs were more evenly distributed on the glass substrates. More

even distribution of SWCNTs was favorable for the formation of conducting network, but contributed to lower visible transmittance as we repeated spin coating. On the PET substrate, an opposite scenario worked. Wetting by the SWCNT-dispersion solution was not as good as on the glass substrates, and SWCNTs were less evenly distributed. Therefore, conducting-network formation was not as easy as on the glass substrates. However, less-even SWCNT distribution resulted in larger void between and within local SWCNT webs, which was favorable for larger transmission. The deviation of the measured values of sheet resistance was less than 5% of the average sheet resistance in the large part of substrates: for example, 70% of the surface of a 2-inch sample. The relatively large difference in sheet resistance at regions near the substrate edge was, presumably, due to large vapor pressure (fast evaporation) of DCE.

Figure 2: Transmittance in visible wavelength range of a series of SWCNT films spin-coated 20, 40, and 100 times, respectively, on (a) glass and (b) PET substrates. Inset shows sheet resistance with respect to transmittance at 550 nm for respective films

One prominent difference between the SWCNT films on the glass and PET substrates was their adhesion to the respective substrates. In spite of the initial good wetting behavior, adhesion of the fabricated SWCNT films on the glass substrates was poor, and SWCNT films were easily detached from the substrates during post-deposition processes, such as nitric-acid treatment. However, the adhesion of SWCNT films on the PET substrates was very good, and SWCNT film remained intact on the substrates, without any special care, during any water-based post-treatments and nitrogen blowing. In order to improve the adhesion between the SWCNTs film and glass substrates, we pretreated the glass-substrate surfaces with 3-aminopropyl triethoxysilane before film casting. First, the 1-wt% solution of 3-aminopropyl triethoxysilane was dropped on the substrates. After 5 minutes, the excess 3-aminopropyl triethoxysilane solution was removed from the substrate by spinning and thoroughly rinsing. Second, a DCB-based SWCNT-dispersion solution was used, instead of the DCE-dispersion solution, to promote the adhesion at the initial stage. Presumably, aromatic benzene rings on the SWCNT sidewall enhance the adhesion between the glass substrate and the SWCNTs when DCB evaporates. However, further study is required to pinpoint the origin of the improved adhesion. Next, the fabricated SWCNT films were subjected to the saturated HNO_3 vapor for 1 hour. Subsequently, the SWCNT films were annealed in a vacuum oven at 80°C for 30min to remove excess water molecules. After repeating the acid treatment and thermal annealing several times, the adhesion between the SWCNT films and glass substrate was dramatically improved so that we could pattern the SWCNT films by using a conventional

photolithography technique. When the same process was applied to the SWCNT films in PET substrates, the adhesion was so good that the SWCNT films could withstand tape or scratch tests without being peeled off.

Acid treatment to reduce sheet resistance of SWCNT films:

Figure 3 shows typical results of post-treatment of the SWCNT films on PET substrates with nitric acid to reduce the sheet resistance. Surprisingly, there was only a very small reduction in visible transmittance, less than 2%, as shown in Fig. 3(a). The reduction in visible transmittance was even smaller for samples showing higher sheet resistance, and concurrently, higher transmittance. Figure 3(b) shows the reduction of normalized sheet resistance with respect to the acid-treatment time. Sheet resistance was reduced to ~50% of the initial value after 1-hour treatment, and remained about the same regardless of the treatment time up to 13.5 hours. However, it appeared that prolonged acid-treatment could damage PET substrates.

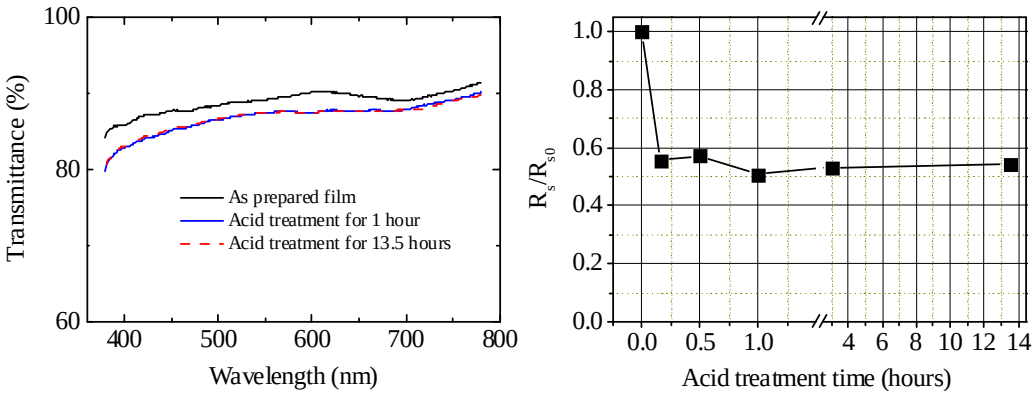

Figure 3: Typical results of post-treatment of SWCNT films on PET substrates with nitric acid: (a) change in transmittance versus wavelength, and (b) reduction of normalized sheet resistance with respect to acid-treatment time

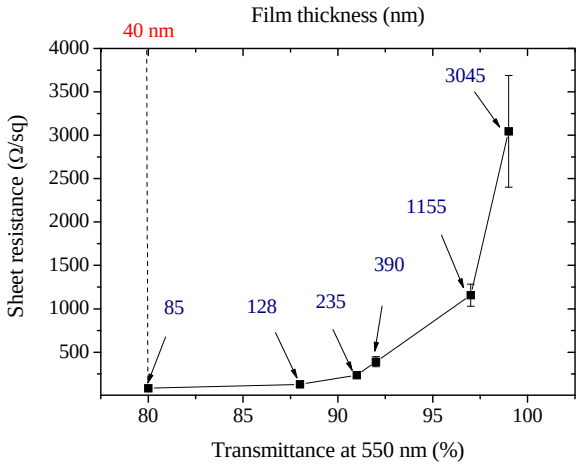

Figure 4: Sheet resistance versus transmittance @ 550nm

Figure 4 shows the sheet resistance with respect to the transmittance at the wavelength of 550nm after the post- treatment with nitric acid. The lowest sheet resistance R_s = 85 Ω/sq at T = 80% appears from the SWCNT film with the thickness of 40 nm, which were

fabricated on a PET substrate by repeating spin coating 300 times. These values of sheet resistance and transmittance are about the same level with those reported by another groups from their chemically treated SWCNT films.

One apparent effect of the acid treatment is the thickness reduction of the SWCNT films. For example, comparison of the thicknesses measured before and after nitric-acid treatment showed that there was 20% reduction in the SWCNT film thickness, from ~50 to ~40 nm, as shown in Fig. 5. Taking into account the thickness reduction together with the reduction of sheet resistance from 222 Ω/sq (as-prepared sample) to 85 Ω/sq, we estimate that there was about 3.3 times improvement in conductivity after the acid treatment. This result is consistent with the report of 2.4 and 3.9 times increase in conductivity after the treatment with $SOCl_2$ and HNO_3, respectively, by other groups. However, the estimated conductivity of our acid-treated sample, 2,940 S/cm, is higher than that of the $SOCl_2$–treated sample, 1,800 S/cm. In the case of another group who also tried nitric-acid treatment, they started from CNT-dispersion solution prepared using the surfactant SDS. They attributed much of their conductivity improvement to the removal of SDS which is an insulating substance. They reported the conductivity increase of 1,500 S/cm together with the 25% film-thickness reduction. It is surprising to find that the thickness reduction and the absolute increase in conductivity of their sample are similar to those of ours. Another benefit of the acid treatment is the surface-morphology improvement, flattening and smoothing, due to the trimming of protruding SWCNTs, as shown in the FESEM images in Figs. 6(a) and 6(b).

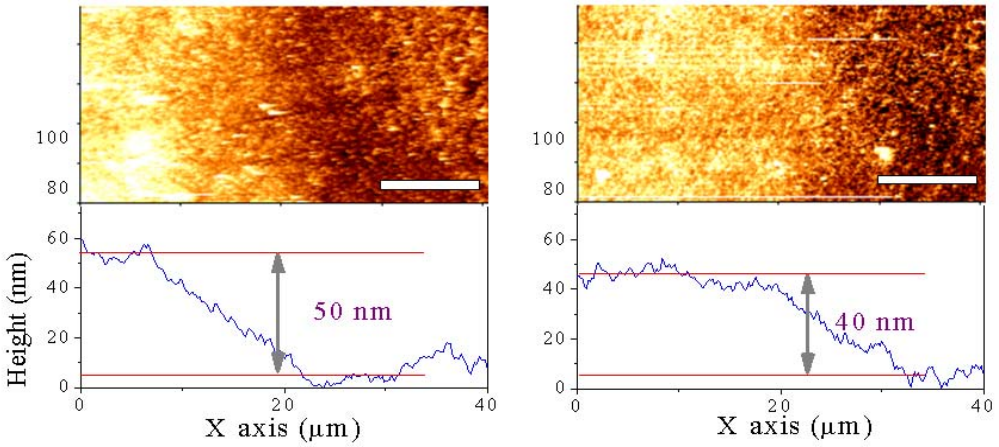

Figure 5: AFM images and line profiles: A change in thickness (a) before, and (b) after acid treatment.

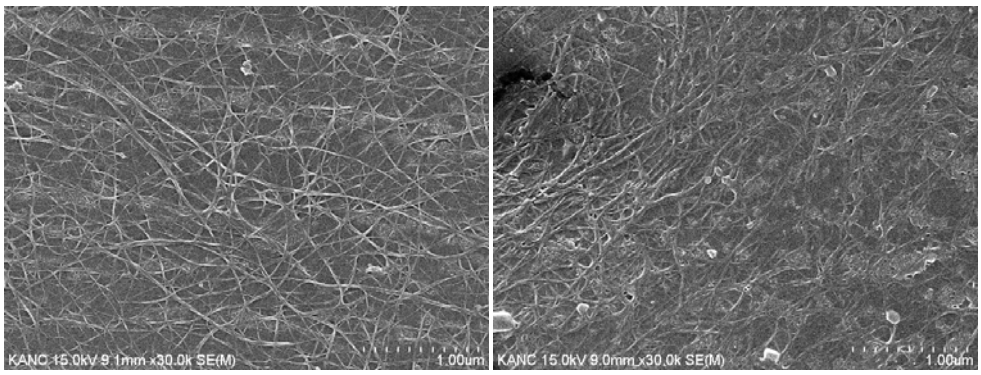

Figure 6: Typical SEM images of SWCNTs film: (a) before, and (b) after acid treatment

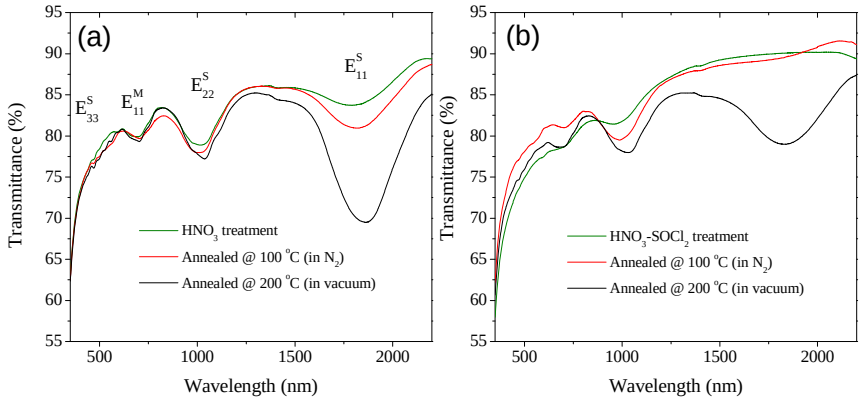

Figure 7: Transmittance versus wavelength in IR-Visible-UV region: (a) HNO_3- and (b) HNO_3-$SOCl_2$ -treated SWCNT films on glass substrates.

Figure 7 shows the van Hove singularities (vHS) of arc-SWCNTs, which appear in the respective absorption spectra of the SWCNTs films treated with HNO_3 or with the combination of HNO_3 and $SOCl_2$. The green solid line in Fig 7(a) corresponds to the as-prepared HNO_3-treated SWCNT film on a glass substrate. The E^S_{11} vHS is substantially suppressed to result in very weak absorption, whereas the E^S_{22} vHS is only slightly bleached. It seems that the dominant effect of the exposure to HNO_3 was the electron withdrawal from the first valence band. However, after annealing this HNO_3-treated SWCNT film at 200 ^oC for 6 hours in vacuum, both vHSs (E^S_{11} and E^S_{22}) are fully recovered; see the black line in Fig. 7(a). The concomitant increase of the sheet resistance by a factor of 6.2 with respect to that of the HNO_3-treated SWCNT film appears as shown in Table 1. On the other hand, the SWCNT film treated with the combination of HNO_3 and $SOCl_2$ shows a complete suppression of the E_{11} vHs together with the deep bleaching of the E_{22} vHs; see the green line in Fig 7(b). This dramatic change in absorption can be attributed to the anodic doping effect (electron withdrawal) that is also responsible for the 60% increase in sheet resistance compared to that of the as-prepared HNO_3-treated film. It is interesting to note that the sheet resistance of the film treated with the combination of HNO_3 and $SOCl_2$ film increased only by a factor of 2.3 after the vacuum annealing at 200 ^oC, whereas the same annealing process induced the sheet-resistance to increase by a factor of 6.2 for the as-prepared HNO_3-treated film. In response to the annealing at 100 ^oC for 1 hour in N_2 atmosphere, which is a typical process to cure PEDOT:PSS during the fabrication of OLEDs and organic solar cells, the sheet resistance of the films treated with HNO_3 or with the combination of $HNO_3$and $SOCl_2$ shows 70% and 40% increase, respectively. These observations indicate that the treatment with the combination of HNO_3 and $SOCl_2$ resulted in more efficient and stable doping compared to the HNO_3–only treatment.

Chemical treatment	Sheet resistance (Ω/sq)		
	As treated	Annealed @ 100 ^oC	Annealed @ 200 ^oC
HNO_3	320	554	1,980
HNO_3-$SOCl_2$	194	286	433

Table 1: Sheet resistance change due to the chemical treatment and annealing

Figure 8 shows the effects of the chemical treatment with either HNO_3 or the combination of HNO_3 and $SOCl_2$ on the Raman spectra of the of SWCNT films. These Raman spectra were measured at the excitation energy of 1.15 eV that is in resonance with the E^S_{22} VHS of arc-SWCNTs. We note that the D and G´ bands are slightly upshifted by 5 and 8 cm^{-1}, respectively, after the HNO_3 treatment, whereas the G bands remains at 1598 cm^{-1} in spite of the acid treatment. This observation is attributed to either the light doping of SWCNTs or to the adsorption of NO_3^- ion on the SWCNT sidewall. On the contrary, a significant displacement of tangential G band to higher frequencies occurs after the HNO_3-$SOCl_2$ combination treatment, which is another evidence for anodic oxidation (or withdrawal of electrons from the SWCNT π band). In this case, the G' band shows a 37-cm^{-1} upshift from 2561 cm^{-1} to 2598 cm^{-1}. The shift of G' band is known as sensitive, in particular, to the carrier density in the π valence band of the SWCNT. The shift of D band to higher frequency was observed, but the intensity of the D band did not change much. The most prominent feature of the Raman spectrum of the SWCNT film treated with the combination of HNO_3 and $SOCl_2$ is the dramatic reduction of the intensity of all the Raman bands because of the loss of resonance at the excitation energy of 1.15eV due to the electron removal from the valence band as clearly manifested in the change of the optical absorption spectra. It is important to note that the effect of heavy doping by the HNO_3-$SOCl_2$ combination treatment can also lead to the downshift of Fermi level as the electron density decreases (or hole density increases).

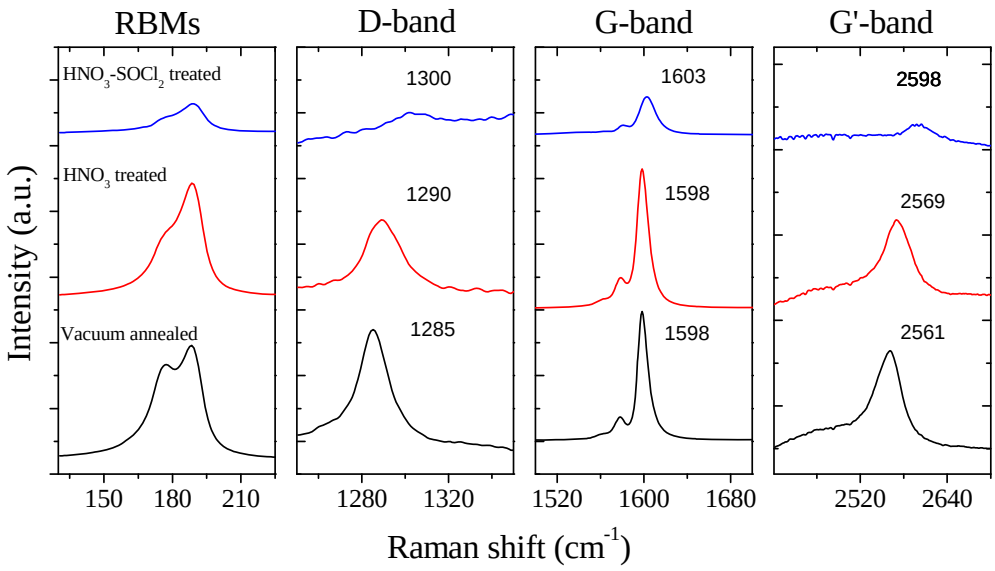

Figure 8: FT-Raman spectra of vacuum-annealed, HNO_3-, and HNO_3-$SOCl_2$-treated SWCNT films on glass substrates

We were able to fit the line-shape of the Raman band around 1600 cm^{-1} by using the Lorentzian function as shown in Fig. 9. The three Lorentzian peaks must be the G^-, G, and G^+ features, respectively, of semiconducting SWCNTs because the Raman spectra were taken under the resonance of the excitation energy (1.15eV) with the E^S_{22} VHS. It is interesting to note that the G-feature of the SWCNT film treated with the combination of HNO_3 and $SOCl_2$

becomes broadened and downshifted because of the heavy doping. However, there is no D* mode, which may originate from the defect on SWCNT sidewall, in all the spectra.

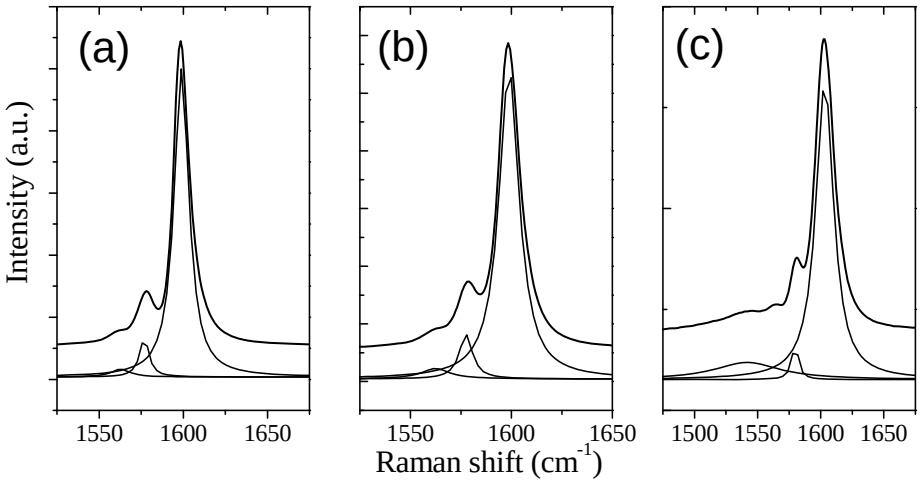

Figure 9: G-bands from the vacuum-annealed (a), HNO_3 treated (b), and HNO_3-$SOCl_2$ treated (c) SWCNT films together with the respective fittings with three Lorentzian peaks.

Figure 10 shows the dependence of the sheet resistance variation on the DI-water exposure time. Initially, there appears a fast sheet-resistance change, 10% increase in response to the 5-minute exposure. However, there is only 20% increase in the sheet resistance after the prolonged exposure up to 240 minutes. This limited sheet-resistance increase is important for the OLED fabrication because DI water is the solvent for PEDOT:PSS that we deposit by spin-coating onto the SWCNT electrode. The typical time for PEDOT:PSS spin-coating is only several minutes, so that we expect less than 10% increase in sheet resistance after the start of the decomposition of chlorine ions.

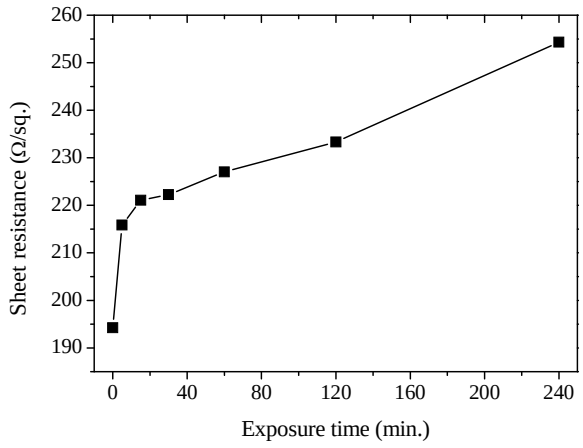

Figure 10: Sheet resistance of $SOCl_2$ treated SWCNTs film with respect to the exposure time to DI water.

Patterning of SWCNT films:

As shown in Fig. 11, we were able to pattern the SWCNT films on either glass- and PET-substrates to form anodes for OLEDs. It is important to emphasize that the patterning process through the conventional photolithography and oxygen-plasma etching induced no degradation in the sheet resistance and transparency of the SWCNT electrodes. Figure 12 shows that the area where the PR covered the surface of the SWCNT film is clean and neat without any PR residue, and that the SWCNT network remains intact without structural damage. Moreover, the root-mean-square (RMS) roughness of the patterned CNT electrode was about 7-10 nm, which is comparable to that of the as-fabricated CNT films.

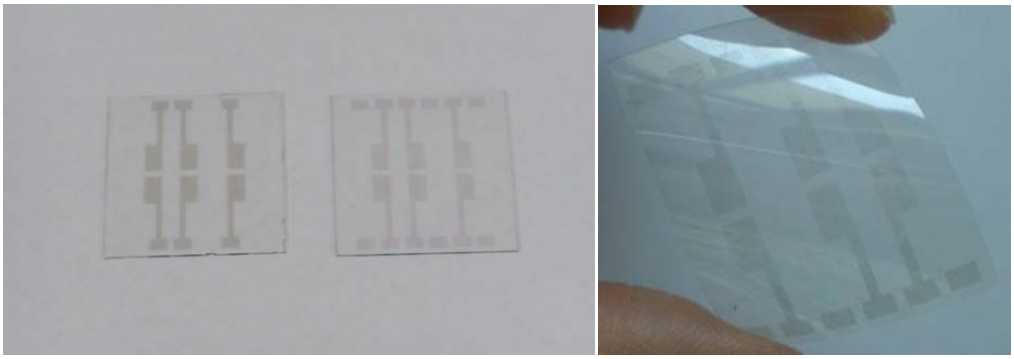

Figure 11: The photographs of patterned SWCNTs film on (a) glass- and (b) PET- substrate.

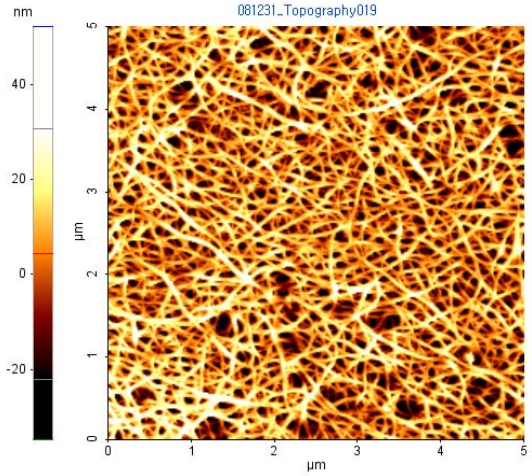

Figure 12: AFM image of patterned SWCNTs film

Fabrication of OLEDs on transparent SWCNT anode

We fabricated a green-emitting OLED using the HNO_3-treated SWCNT film on a glass substrate, having the sheet resistance of 125 Ω/sq and visible-light transmittance of ~75%, as an anode. The thickness of this SWCNT film was 30 nm as shown in Fig. 13, and its conductivity was 2,666 S/cm, a little smaller than that of the best SWCNT film. We tested the thermal stability of this HNO_3-treated SWCNT film because the OLED fabrication involves a heat-treatment process for a PEDOT:PSS layer that is used as a planarization and hole injection layer. Surface planarization is essential, in particular, for an anode having rough surface, such as the SWCNT film. As it turned out, sheet resistance of the SWCNT film doubled compared to that of the as-maid HNO_3-treated film. It is clear from Fig. 13(b) that

the most of the suppression of the S_{11} transition (1600nm-2000nm) in the HNO_3-treated SWCNT film is recovered by baking the SWCNT film at 100 °C for 1 hour. We attribute the recovery of the S_{11} transition to the de-doping of NO_3^- molecules due to the heating process.

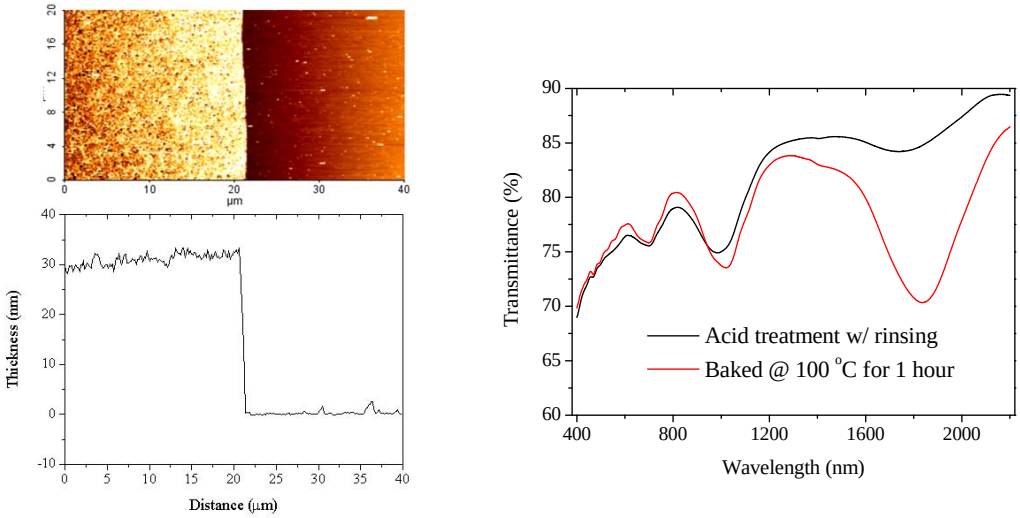

Figure 13: AFM image and line profile of the HNO_3-treated SWCNT film, and the comparison of the visible transmittance of the acid-treated and baked SWCNT films.

The layer structure of the green-emitting OLED that we fabricated using the SWCNT film on a glass substrate was SWCNT-anode/PEDOT:PSS(90 nm)/NPB(200 nm)/Alq_3(40 nm)/LiF(1 nm)/Al(100 nm). As usual, the PEDOT:PSS and NPB layers were used as a HIL and a HTL, respectively, and the Alq_3 layer adjacent to a composite cathode of LiF/Al was a green-emitting EML. Figure 14 shows that the RMS roughness of the patterned SWCNT anode was reduced substantially, down to less than 2 nm, after the deposition of the PEDOT:PSS layer. 2-nm RMS roughness is only slightly higher than that of a typical PEDOT:PSS layer on an ITO glass.

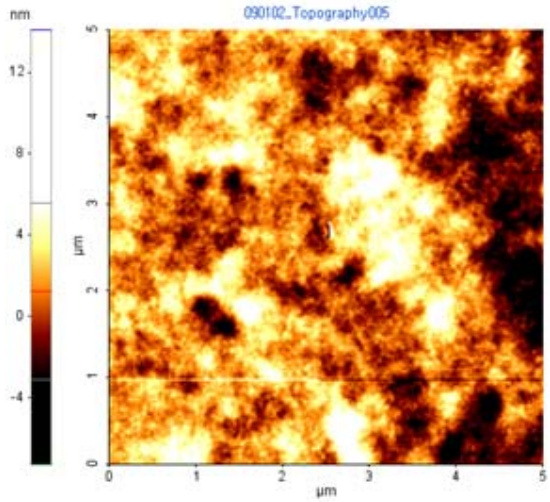

Figure 14: AFM image of PEDOT:PSS coated SWCNT film

The current and luminance of the fabricated green-emitting device with respect to the applied bias-voltage are shown in Fig. 15. The luminance of 1700 cd/m^2 and the current density of 100mA/cm^2 were measured at the bias of ~6.5 V. The luminance yield of 1.76 cd/A (@100mA/cm^2) is about half of that of a similar device with an ITO anode. The EL (electroluminescence) spectra from this device have the peak at 532 nm, and there is no voltage-dependent shift of the peak position as shown in Fig. 16. The peak position with no voltage dependence indicates that electron-hole recombination occurred only in the Alq_3 EML. Internationale de l'Eclairage chromaticity coordinates $CIE_{x,y}$ of the spectra is (0.32, 0.52) that is very similar (or identical) to the color coordinates of conventional Alq_3 OLEDs.

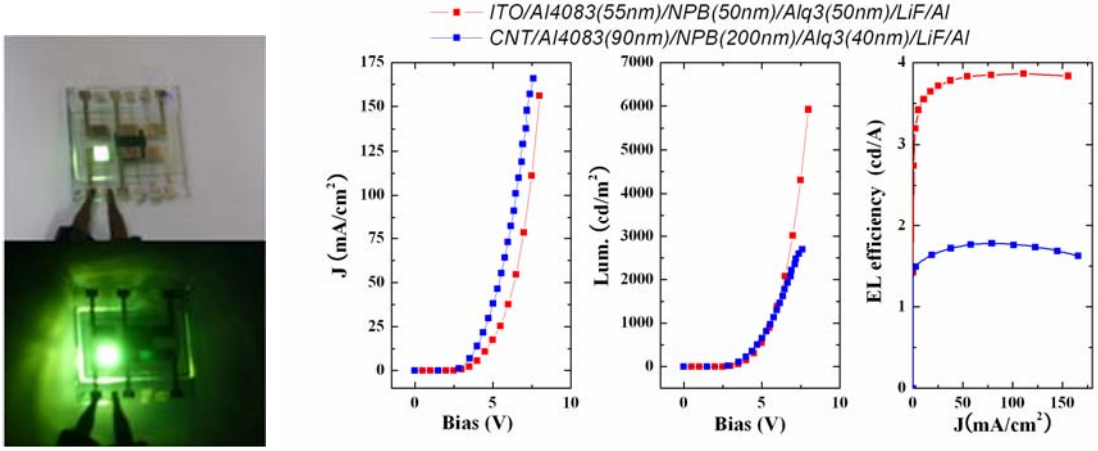

Figure 15: Photographs of the OLED with a SWCNT anode and an Alq_3 EML in operation and the corresponding current and luminance characteristics with respect to the applied bias voltage.

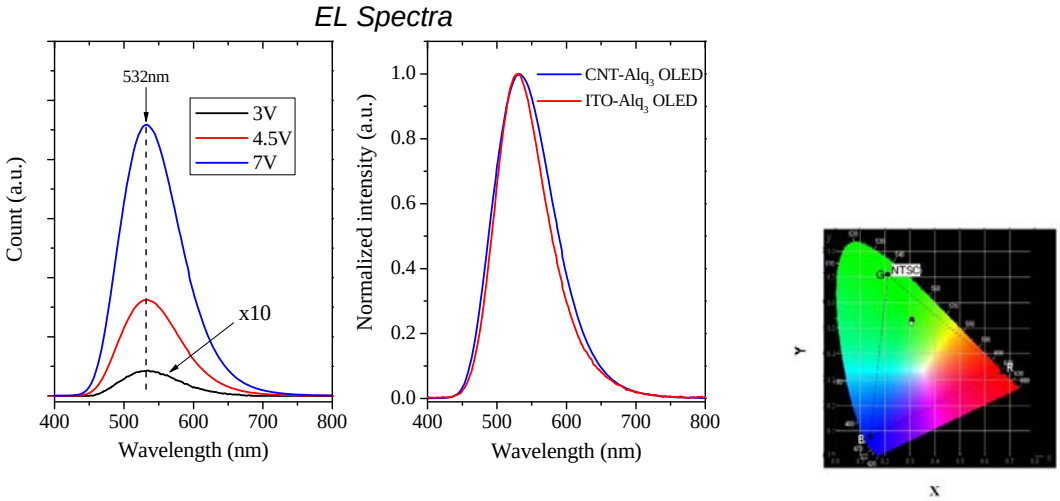

Figure 16: EL spectra of Alq3-OLEDs and CIE color coordinates.